JOM, Vol. 73, No. 2, 2021
https://doi.org/10.1007/s11837-020-04527-4

Gold Solubility in $CaO-SiO_2-Al_2O_3-Fe_2O_3$ Slags

JUN GIL YANG,[1] JOO HO PARK,[1] JI YEON KANG,[1] HYUN SIK PARK,[2] and JOO HYUN PARK [1,3,4]

1.—Department of Materials Science and Chemical Engineering, Hanyang University, Ansan 15588, Korea. 2.—Resources Recovery Research Center, Korea Institute of Geoscience and Mineral Resources (KIGAM), Daejeon 34132, Korea. 3.—Department of Materials Science and Engineering, KTH Royal Institute of Technology, 100 44 Stockholm, Sweden. 4.—e-mail: basicity@hanyang.ac.kr

Gold solubility in the $CaO-SiO_2-Al_2O_3-Fe_2O_3$ slag system was measured at 1723 K under an oxidizing atmosphere. Gold solubility in the present slag system increased with increasing slag basicity, which was quantified by the Vee ratio (= CaO/SiO_2), theoretical optical basicity, and activity of CaO. However, the effect of Fe_2O_3 and Al_2O_3 on gold solubility was negligible. From the thermodynamic assessment, it was found that gold was stabilized as the AuO^- (*aurate*) complex ion, and thus the dissolution reaction into the slag was proposed. The *aurate capacity* was originally defined from the dissolution reaction. The iso-Au solubility contours were plotted in the $CaO-Fe_2O_3-(SiO_2 + Al_2O_3)$ pseudo-ternary diagram, from which the lower content of CaO can be proposed to be useful for higher recovery of gold (i.e., lower solubility) based on the thermodynamic view during pyrometallurgical processing of gold-containing E-waste materials. However, because the viscosity of the slag increases by decreasing the content of CaO, the operating window for best practice should be carefully proposed by considering the physicochemical properties of molten slag.

INTRODUCTION

Gold is a bright and slightly reddish yellow and is one of the most malleable and ductile metals. It has been used for coinage, jewelry, and other arts throughout recorded history.[1] Chemically, gold is unaffected by most acids, such as hydrochloric, sulfuric, and nitric acid. Also, it does not react with water, dry or humid air, and most corrosive reagents.[2] Because gold has good physicochemical properties, it is one of the most important noble metals with wide applications in industrial and economic activities. For example, over 300 tons of gold are used annually in electronic components such as electroplated coatings on connectors and contacts in electrical devices.[2]

Thus, the gold price in the market has increased rapidly, and some researchers have studied the recycling technology of gold-containing (electrical and electronic wastes, E-wastes) materials.[2] Several previous studies reported the distribution ratio of gold between slag, matte, and metal or the solubility of gold in pyrometallurgical slags in view of the applications in non-ferrous smelting processes as well as in E-waste recycling processes.[3–12] An integrated literature review regarding the gold dissolution behavior into the metallurgical slags is available in our previous article.[9] In the present study, we measured the gold solubility in the $CaO-SiO_2-Al_2O_3-Fe_2O_3$ slag syste m at 1723 K under an atmospheric condition to determine the dissolution behavior of gold with varying slag composition. The gold dissolution behavior was also investigated by employing the various basicity indices.

(Received August 26, 2020; accepted December 5, 2020; published online January 15, 2021)

EXPERIMENTAL PROCEDURE

Thermochemical equilibration experiments were carried out using a super kanthal electric resistance furnace with a $MoSi_2$ heating element. A schematic diagram of the experimental apparatus is available in our previous articles.[9,13–16] The temperature was controlled within ± 2 K using a B-type (Pt-30%Rh/Pt-6%Rh) thermocouple and a proportional integral

differential controller. Pure gold (99.99% purity) was used, and slag samples were prepared by mixing reagent-grade SiO_2, Al_2O_3, Fe_2O_3, and CaO calcined from $CaCO_3$ at 1273 K for 10 h.

Gold (0.5 g) and slag (3 g) were loaded into a fused alumina (99.9% purity) crucible (18 mm-∅ × 14 mm-∅ × 50 mm-H) placed in a porous alumina holder (50 mm-∅ × 45 mm-∅ × 70 mm-H) and maintained at 1723 K under atmospheric conditions. After 24 h of equilibration, which was determined in preliminary experiments, the samples were quickly extracted from the furnace and quenched by plunging the crucible into brine. Then, the slag and gold were carefully separated from the crucible. The interface between gold and slag was clearly defined and allowed a clean separation as shown in Fig. 1. The morphology and chemistry of the separated gold were characterized by field emission scanning electron microscopy (FE-SEM, MIRA3; TESCAN, Czech Republic) with an energy dispersive x-ray spectroscope (EDS) at an operating voltage of 15 kV.

The slag was ground to fine powder for chemical analysis. The gold content in the slag was analyzed by inductively coupled plasma-optical emission spectroscopy (ICP-OES, iCAP6500; Thermo Scientific, Waltham, MA), and the equilibrium composition of the slag was analyzed using an x-ray fluorescence spectroscopy (XRF, S4 Explorer; Bruker AXS Inc., Madison, WI). Furthermore, the content of ferrous (Fe^{2+}) ion in slag samples was determined by titration method using potassium dichromate (KS E 3016:2003).[13,17] From the analysis results, it was confirmed that 'Fe' could be mainly stabilized as ferric ion, Fe^{3+} (i.e., Fe_2O_3), in the present slag system under atmospheric conditions, viz. $p(O_2)$ = 0.21 atm. The entire experimental results are listed in Table I.

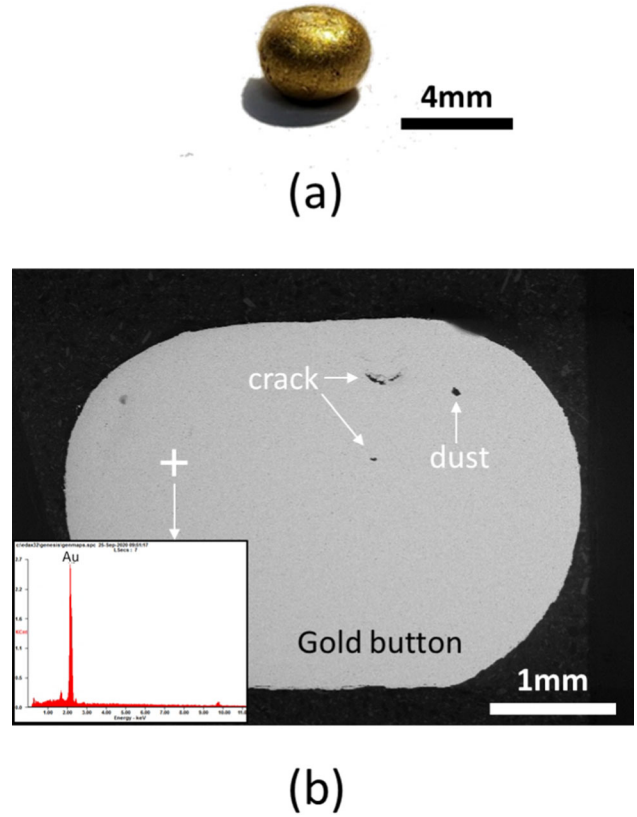

Fig. 1. (a) Morphology of a gold button separated from the slag and (b) vertical section of the gold button in back-scattered electron image with the EDS spectrum.

RESULTS AND DISCUSSION

The gold dissolution reaction into the CaO-based slag was proposed by the following equation:[9]

$$\mathrm{Au}(l) + \frac{1}{4}\mathrm{O_2}(g) + \frac{1}{2}\left(\mathrm{O^{2-}}\right) = (\mathrm{AuO^-}) \quad (1)$$

$$K_{(1)} = \frac{a_{\mathrm{AuO^-}}}{a_{\mathrm{Au}} \cdot p_{\mathrm{O_2}}^{1/4} \cdot a_{\mathrm{O^{2-}}}^{1/2}} = \frac{f_{\mathrm{AuO^-}} \cdot (\%\mathrm{AuO^-})}{p_{\mathrm{O_2}}^{1/4} \cdot a_{\mathrm{O^{2-}}}^{1/2}} \quad (2)$$

where $K_{(1)}$, a_i, f_i, and $p_{\mathrm{O_2}}$ are the equilibrium constant of Eq. 1, activity and the activity coefficient of component i, and the oxygen partial pressure, respectively. As shown in Fig. 1b, there were no impurity elements under EDS detection limit (approximately 0.01 wt.%), and none of second phase particles were observed in gold. As the standard state of gold is taken as the pure liquid gold at experimental temperature, the activity of gold can be assumed to be unity. Therefore, Eq. 2 can be expressed as follows:

$$\log(\%\mathrm{AuO^-}) = \frac{1}{2}\log a_{\mathrm{O^{2-}}} + \frac{1}{4}\log p_{\mathrm{O_2}} - \log f_{\mathrm{AuO^-}} + \mathrm{Const.} \quad (3)$$

From Eq. 3, the solubility of gold is expected to have a linear function with the activity of O^{2-} ion, viz., basicity at a fixed temperature and oxygen partial pressure on a logarithmic scale. Because the activity of free oxygen cannot be directly measured because of thermodynamic constraints, a number of measures for slag basicity such as the (modified) Vee ratio, optical basicity, activity of basic oxide, and so on, have been proposed as an indirect basicity index.[9,13,14,18–20]

To define the (modified) Vee ratio in the CaO-SiO_2-Al_2O_3-Fe_2O_3 slag system, the effect of slag components, viz. Al_2O_3 and Fe_2O_3, on the solubility of gold at 1723 K are shown in Figs. 2 and 3. The solubility of gold in the present slag system slightly decreases (but not significant) with increasing content of Al_2O_3, while it is independent of Fe_2O_3 content. The effect of Al_2O_3 on gold solubility in the CaO-SiO_2-Al_2O_3-MgO slag at 1773 K, which is available in the literature,[9] is also shown in Fig. 2 for the sake of comparison.

The Al_2O_3 dependency of gold solubility in the CaO-SiO_2-Al_2O_3-MgO slag system is nearly the same as that in the present Fe_2O_3-containing

Table I. Experimental results in the present study

Run number	Content (wt.%)					Content of Au (ppm)
	CaO	SiO_2	Al_2O_3	Fe_2O_3	FeO	
1	30.6	20.0	18.2	29.6	1.6	40.5 (± 2.2)
2	25.1	27.1	32.1	14.4	1.3	25.4 (± 1.5)
3	27.3	32.4	26.5	12.7	1.1	21.2 (± 1.3)
4	29.6	21.1	26.6	21.2	1.4	30.4 (± 1.7)
5	25.2	23.4	27.1	22.6	1.7	27.8 (± 1.6)
6	26.2	18.5	23.2	29.5	2.6	32.1 (± 1.8)
7	19.7	23.2	24.5	29.4	3.3	26.2 (± 1.5)
8	15.7	29.2	31.4	20.9	2.8	16.2 (± 1.0)

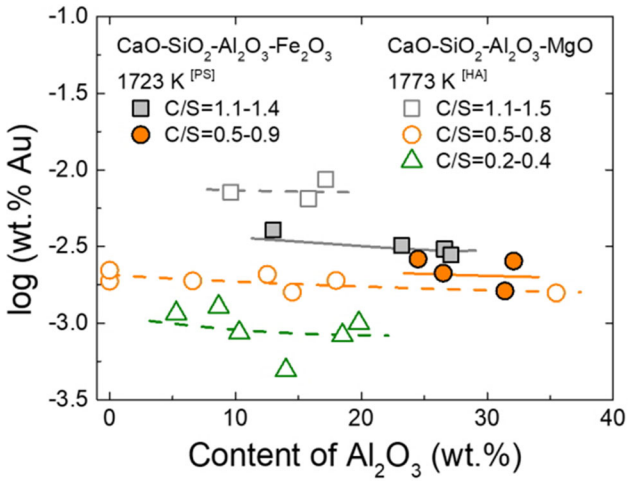

Fig. 2. Effect of Al_2O_3 content on gold solubility in the CaO-SiO_2-Al_2O_3-Fe_2O_3 slag at 1723 K ([PS]: present study, [HA]: Han et al.[9]).

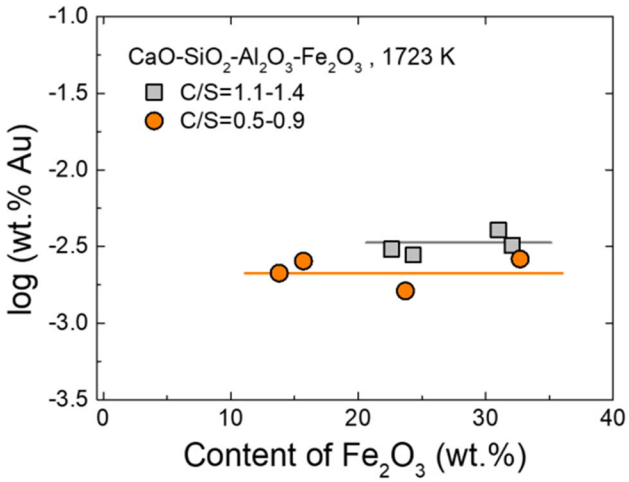

Fig. 3. Effect of Fe_2O_3 content on gold solubility in the CaO-SiO_2-Al_2O_3-Fe_2O_3 slag at 1723 K.

oxidizing slag system. Comparing the gold solubility in MgO- and Fe_2O_3-bearing slags with C/S > 1.0, the gold solubility in the former system is slightly

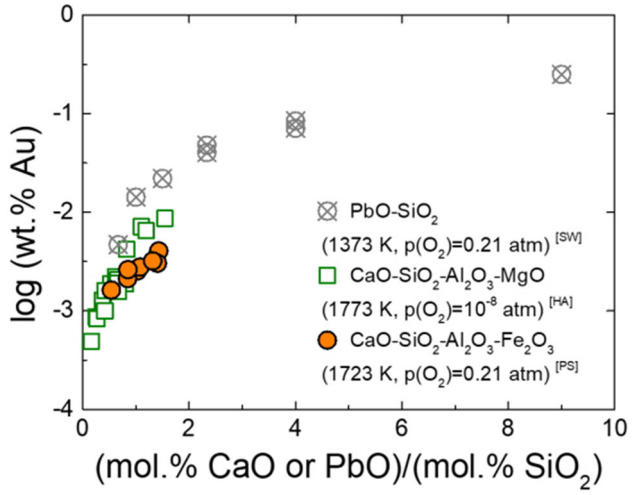

Fig. 4. Effect of (mol% CaO or PbO)/(mol% SiO_2) ratio on gold solubility in CaO slags and PbO slag ([PS]: present study, [HA]: Han et al.[9], [SW]: Swinbourne et al.[8]).

larger than that in the latter system. This means that MgO behaves as a more basic component than Fe_2O_3 does in the CaO-based slags. However, the difference in gold solubility between MgO- and Fe_2O_3-bearing slags is negligible when the C/S ratio is < 1.0. The more specific discussion regarding the influence of slag composition on gold solubility is given as follows.

Consequently, from the experimental results shown in Figs. 2 and 3, it is concluded that Fe_2O_3 and Al_2O_3 are not necessarily included in basicity index in the present study, which means that just the Vee ratio (= CaO/SiO_2 ratio) is enough to investigate the influence of basicity on gold solubility in the present study. The solubility of gold in the CaO-SiO_2-Al_2O_3-Fe_2O_3 slag at 1723 K and $p(O_2)$ = 0.21 atm is plotted against the Vee ratio in Fig. 4. The gold solubility in the CaO-SiO_2-Al_2O_3-MgO slag at 1773 K and $p(O_2) = 10^{-8}$ atm measured by Han et al.[9] and that in the PbO-SiO_2 slag at 1373 K and $p(O_2)$ = 0.21 atm measured by Swinbourne et al.[8] are also shown in Fig. 4. The gold solubility in the

CaO-based slags and $PbO\text{-}SiO_2$ slag commonly increases with increasing Vee ratio (PbO is considered as a basic oxide in the latter). Furthermore, the gold solubility in the PbO slag is slightly higher than that in the CaO slag at a given MO (M = Ca and Pb) content, which possibly originated from the lower temperature and higher oxygen potential in the former.[9] From Eq. 1, it is noticeable that the gold solubility increases with increasing oxygen potential, which means that the gold dissolution reaction is exothermic and hence is promoted at lower temperatures. The more specific discussion regarding the effects of oxygen potential and temperature on the gold dissolution behavior in the slag is available in our previous article.[9]

An optical basicity has widely been used as a quantitative measure of the basicity of slags and glasses to evaluate the influence of slag composition on the physicochemical properties of oxide melts since it was originally defined by Duffy and Ingram.[21,22] The optical basicity concept is based on the electron donor power of single oxide component, and the theoretical optical basicity of the melts can be calculated from Eq. 4 using the basicity value of the pure component as listed in Table II.[21–23]

$$\Lambda_{\text{melt}} = \frac{\sum X_i \cdot n_i \cdot \Lambda_i}{\sum X_i \cdot \Lambda_i} \tag{4}$$

where X_i, n_i, and Λ_i are the mole fraction of oxide, amount of oxygen in each oxide, and theoretical optical basicity of pure component i, respectively. The gold solubilities in the CaO-based and PbO-based slags are plotted against the optical basicity of the melts in Fig. 5. There are relatively good linearities between log (wt.% Au) and optical basicity of the melts ranging from 0.6 to 0.9, which means that the optical basicity can be employed as a good basicity index for quantifying the gold solubility in the CaO- and PbO-based (alumino-)silicate melts.

As mentioned earlier, the basicity of molten slag can be approximated to the activity of basic oxide, for example, CaO, at fixed temperature and oxygen partial pressure assuming that the activity of CaO is in proportion to that of O^{2-} ion by the following equations.

$$(\text{CaO}) = \left(\text{Ca}^{2+}\right) + \left(\text{O}^{2-}\right) \tag{5}$$

$$K_{(5)} = \frac{a_{\text{Ca}^{2+}} \cdot a_{\text{O}^{2-}}}{a_{\text{CaO}}} \tag{6}$$

By combining Eqs. 3 and 6, Eq. 7 can be deduced.

$$\log(\%\text{AuO}^-) = \frac{1}{2}\log a_{\text{CaO}} - \frac{1}{2}\log a_{\text{Ca}^{2+}} - \log f_{\text{AuO}^-} + \frac{1}{4}\log p_{\text{O}_2} + \text{Const.} \tag{7}$$

Table II. Theoretical optical basicity of pure oxide component[21–23]

Oxide	Optical basicity, Λ_i
CaO	1.00
SiO_2	0.48
Al_2O_3	0.61
MgO	0.78
Fe_2O_3	0.75
PbO	0.96

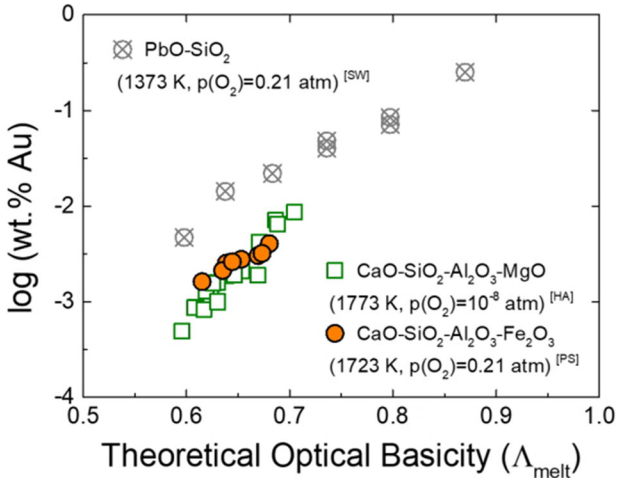

Fig. 5. Relationship between gold solubility and theoretical optical basicity in CaO slags and PbO slag ([PS]: present study, [HA]: Han et al.,[9] [SW]: Swinbourne et al.[8]).

Hence, the solubility of gold is expected to be proportional to the activity of CaO with a slope of 1/2 assuming that the activity of Ca^{2+} and the activity coefficient of AuO^- species are not seriously affected by the slag composition at a fixed temperature and oxygen partial pressure. These assumptions are thermodynamically feasible not only because Ca^{2+} ions are mainly charge-balanced with non-bridging oxygen ions (O^-) in the aluminosilicate melts but also because AuO^- ions are expected to exhibit a Henrian behavior in an infinite dilution condition in the slag melts.[9,13–20,24,25] In the present study, the activity of CaO in the $CaO\text{-}SiO_2\text{-}Al_2O_3\text{-}Fe_2O_3$ slag was calculated by FactSage™7.3 (ESM software, Hamilton, OH), which is a commercial thermochemical computing program.[26] This software has been successfully used for computing the gas-slag-metal multiphase equilibria in ferrous and non-ferrous metallurgical systems.[9–20,24–29]

The relationship between gold solubility and CaO activity in the $CaO\text{-}SiO_2\text{-}Al_2O_3\text{-}Fe_2O_3$ slag at 1723 K is shown in Fig. 6. A good linear correlation between them on a logarithmic scale can be found with the slope of 0.36 (± 0.025) (r^2 = 0.96), which

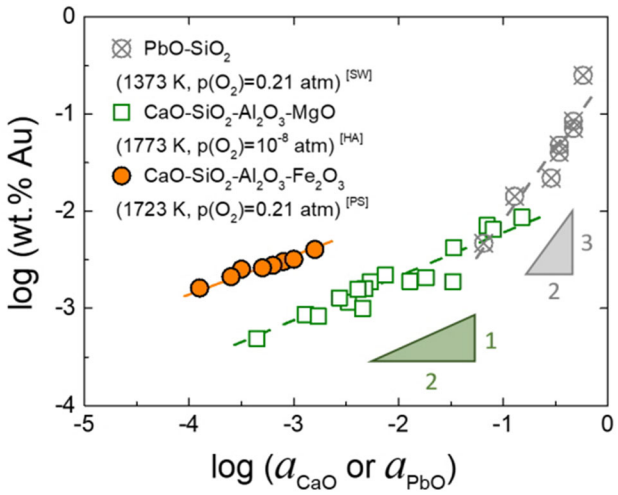

Fig. 6. Dependence of gold solubility on the activity of CaO and PbO in CaO slags and PbO slag ([PS]: present study, [HA]: Han et al.[9], [SW]: Swinbourne et al.[8]).

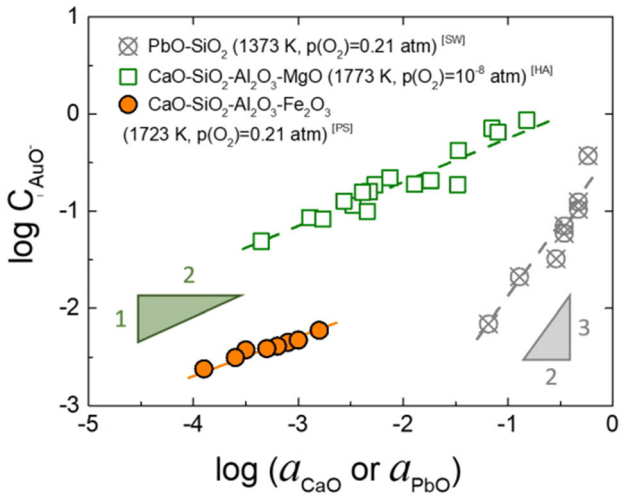

Fig. 7. Dependence of *aurate capacity* on the activity of CaO and PbO in CaO slags and PbO slag ([PS]: present study, [HA]: Han et al.[9], [SW]: Swinbourne et al.[8]).

was obtained from a linear regression analysis. Even though there are some experimental scatters, the slope of the fitted line is approximately close to 0.5. A discrepancy between theoretical slope and measured one possibly originated from the changes in the activity of Ca^{2+} and/or the activity coefficient of AuO^- according to the slag composition. A similar relationship was also reported in the CaO-SiO_2-Al_2O_3-MgO slag system at 1773 K in our earlier work.[9]

From the above results, the ionic dissolution reaction in Eq. 1 can be employed to the present oxidizing slag system. The details for the dissolution mechanism of gold in the PbO-based melts are available in previous articles.[8,9] The solubility of gold in the CaO-SiO_2-Al_2O_3-Fe_2O_3 slag is higher than that in the CaO-SiO_2-Al_2O_3-MgO slag at a given CaO activity, because the gold solubility in the former was measured under highly oxidizing atmosphere and lower temperature.[9]

To quantify the influence of slag composition on the thermodynamic behavior of gold in the slags irrespective of oxygen potential variable, the *aurate capacity* (as likely as the phosphate capacity) can be employed as follows. From the dissolution reaction of gold, which is given in Eq. 1, the *aurate capacity* of the slag can be defined as follows.

$$C_{AuO^-} = \frac{K_{(1)} \cdot a_{O^{2-}}^{1/2}}{f_{AuO^-}} = (\%AuO^-) \cdot p_{O_2}^{-1/4} \qquad (8)$$

Combining Eqs. 6 and 8, the following relationship can be deduced.

$$\log C_{AuO^-} = \frac{1}{2}\log a_{CaO} - \frac{1}{2}\log a_{Ca^{2+}} - \log f_{AuO^-} + \text{Const.} \qquad (9)$$

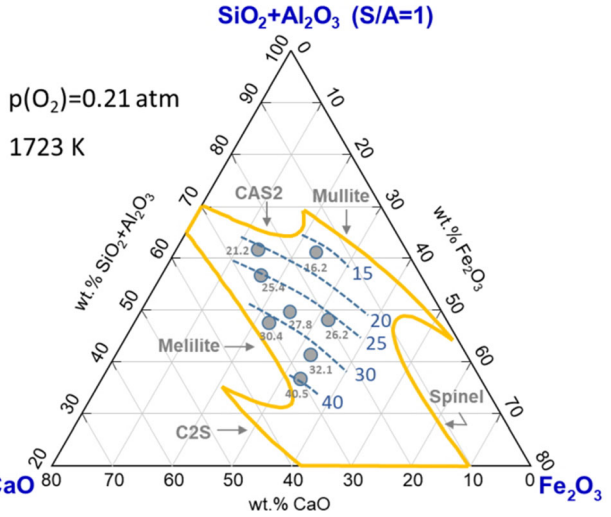

Fig. 8. Iso-Au solubility (ppm) contours in the CaO-SiO_2-Al_2O_3-Fe_2O_3 slag at 1723 K (C: CaO, S: SiO_2, A: Al_2O_3). Phase diagram was calculated using FactSage™7.3.

The relationship between *aurate capacity* and the activity of CaO and PbO in the CaO-based and PbO-based slags, respectively, is shown in Fig. 7. The *aurate capacity* of the CaO-SiO_2-Al_2O_3-MgO slag at 1773 K is greater than that of the CaO-SiO_2-Al_2O_3-Fe_2O_3 slag at 1723 K and that of the PbO-SiO_2 slag at 1373 K at a given MO (MO = CaO or PbO) activity because the CaO-SiO_2-Al_2O_3-MgO slag is unambiguously more basic than the others. The details for the dissolution behavior of gold in PbO slag is available elsewhere.[8,9]

The iso-gold solubility (ppm) contours in the CaO-SiO_2-Al_2O_3-Fe_2O_3 slag system at 1723 K under an atmospheric condition, i.e., $p(O_2)$ = 0.21 atm, are

shown in Fig. 8. Here, SiO_2 and Al_2O_3 are merged for the sake of simplicity in the pseudo-ternary diagram. The gold solubility in the present slag system increases with increasing amounts of CaO, whereas the influence of Fe_2O_3 on the solubility of gold is negligible. Hence, the high-SiO_2 slag is better than high-CaO slag in view of chemical dissolution (loss) of gold into the slag based on thermodynamics. However, the viscosity drastically increases with increasing content of SiO_2, resulting in a decrease in the falling-down velocity of metal droplets in the slag phase based on Stoke's law.[24,25,30,31] Thus, the high-CaO slag is better than high-SiO_2 slag in view of the physical loss of gold based on fluid dynamics. Consequently, the optimum window for best practice operation should be recommended by considering the physicochemical properties of molten slag during pyrometallurgical processing of E-waste materials to obtain a high yield (or recovery) of gold.

CONCLUSION

The gold solubility in the CaO-SiO_2-Al_2O_3-Fe_2O_3 slag was measured at 1723 K under an atmospheric condition, i.e., $p(O_2) = 0.2$ atm. Gold solubility in the slag was evaluated as a function of various basicity indices, viz., the Vee ratio (= CaO/SiO_2 ratio), optical basicity, and the activity of CaO. From the thermodynamic analysis, the following gold dissolution reaction into the present Fe_2O_3-containing oxidizing slag was confirmed, and thus the *aurate capacity* was originally defined from the equilibrium constant of this reaction.

$$\mathrm{Au}(l) + \frac{1}{4}\mathrm{O}_2(g) + \frac{1}{2}\left(\mathrm{O}^{2-}\right) = \left(\mathrm{AuO}^{-}\right)$$

Combining the present and the previous results, one can design the slag system to minimize the gold loss to slag phase (i.e., maximizing the gold recovery to the base metal bath) during pyrometallurgical processing of gold-containing E-wastes. That is, the excess addition of basic oxides such as CaO and MgO is not recommended. However, high-SiO_2 slags are highly viscous, resulting in slow kinetics of the slag-metal reaction as well as a slow falling rate of metallic particles during the process. Consequently, the physicochemical properties of slag should be carefully considered.

ACKNOWLEDGEMENTS

This research was partly supported by the R&D Center for Valuable Recycling (Global-Top R&BD Program, Grant No. 2019002220002), funded by the Ministry of Environment (MOE), Korea. This research was also partly supported by the Competency Development Program for Industry Specialists (Grant No. P0002019), funded by the Ministry of Trade, Industry and Energy (MOTIE), Korea.

CONFLICT OF INTEREST

On behalf of all authors, the corresponding author states that there is no conflict of interest.

REFERENCES

1. F. Habashi, *Encyclopedia of Metalloproteins*, 2014, p. 932.
2. C. Hageluken and C.W. Corti, *Gold Bull.* 43, 209 (2009).
3. J.P. Hager, S.M. Howard, and J.H. Jones, *Metall. Trans.* 1, 415 (1970).
4. R. Altman and H.H. Kellogg, *Miner. Process. Ext. Metall. (Trans. Inst. Min. Metall. C)* 81C, 163 (1972).
5. M. Nagamori and P.J. Mackey, *Metall. Trans. B* 9B, 567 (1978).
6. H. Asao and K. Kamiya, *Adv. Compos. Mater.* 12, 1 (2003).
7. B.S. Kim, J.C. Lee, S.P. Seo, Y.K. Park, and H.Y. Sohn, *JOM* 56, 55 (2004).
8. D.R. Swinbourne, S. Yan, and S. Salim, *Min. Process. Extract. Metall. (Trans. Inst. Min. Metall. C)* 114C, 23 (2005).
9. Y.S. Han, D.R. Swinbourne, and J.H. Park, *Metall. Mater. Trans. B* 46B, 2449 (2015).
10. M.A.H. Shuva, M.A. Rhamdhani, G.A. Brooks, S. Masood, and M.A. Reuter, *J. Clean. Prod.* 131, 795 (2016).
11. D. Shishin, T. Hidayat, J. Chen, P.C. Hayes, and E. Jak, *J. Sustain. Metall.* 5, 240 (2019).
12. N. Hellstén, L. Klemettinen, D. Sukhomlinov, H. O'Brien, P. Taskinen, A. Jokilaakso, and J. Salminen, *J. Sustain. Metall.* 5, 463 (2019).
13. J.H. Heo, S.S. Park, and J.H. Park, *Metall. Mater. Trans. B* 43B, 1098 (2012).
14. Y.S. Han and J.H. Park, *Metall. Mater. Trans. B* 46B, 235 (2015).
15. E.H. Jeong, C.W. Nam, K.H. Park, and J.H. Park, *Metall. Mater. Trans. B* 47B, 1103 (2016).
16. J.G. Yang and J.H. Park, *Metall. Mater. Trans. B* 48B, 2147 (2017).
17. T.S. Kim and J.H. Park, *J. Non-Cryst. Solids* 542, 120089 (2020).
18. N. Sano, *Advanced Physical Chemistry for Process Metallurgy* (San Diego: Academic Press, 1997), p. 46.
19. J.H. Park, G.H. Park, and Y.E. Lee, *ISIJ Int.* 50, 1078 (2010).
20. J.H. Park and D.J. Min, *Metall. Mater. Trans. B* 30B, 689 (1999).
21. J.A. Duffy and M.D. Ingram, *Phys. Chem. Glasses* 16, 119 (1975).
22. J.A. Duffy, M.D. Ingram, and I.D. Sommerville, *J. Chem. Soc. Faraday Trans. I* 74, 1410 (1978).
23. K.C. Mills and S. Sridhar, *Ironmak. Steelmak.* 26, 262 (1999).
24. J.H. Park, *J. Non-Cryst. Solids* 358, 3096 (2012).
25. J.H. Park, *Met. Mater. Int.* 19, 577 (2013).
26. FactSage, www.factsage.com. Accessed 1st July 2020.
27. J.H. Park, M.O. Suk, I.H. Jung, M. Guo, and B. Blanpain, *Steel Res. Int.* 81, 860 (2010).
28. J.H. Heo, Y. Chung, and J.H. Park, *J. Clean. Prod.* 137, 777 (2016).
29. S.K. Kwon, J.S. Park, and J.H. Park, *ISIJ Int.* 55, 2589 (2015).
30. J.H. Heo, B.S. Kim, and J.H. Park, *Metall. Mater. Trans. B* 44B, 1352 (2013).
31. H.S. Park, Y.S. Han, and J.H. Park, *ACS Sustain. Chem. Eng.* 7, 14119 (2019).